Design and Optimization of the Flexible Support Structure for Space Mirror

Yixuan Sun[✉], Shikui Luo, Jie Bai, Zijia Liu, and Shaofan Tang

Beijing Institute of Space Mechanics and Electricity, Beijing 100094, China
`sundae90@126.com`

Abstract. The mirror subassembly is the key component of the space optic remote sensor and the mirror shape is always required to reach high accuracy due to the crucial importance to the system's imaging quality. However, the mirror shape is usually influenced by gravity, temperature, forced displacement and launch vibrations to distort after leaving earth. The support structure of the subassembly plays an important role to minimize the impact of above factors while the conflict of the mirror's static accuracy and the subassembly's dynamic strength needs to be studied. Therefore, based on a Φ 260 mm-aperture mirror subassembly, a whole set of flexible support structures was researched. Combining with the conventional ring-type lateral support structure, a discrete-type flexible mounting scheme was proposed. Materials of the mirror and cell, the micro-stress mounting strategy and parameters of the flexure hinges were established aiming at maintaining high static precision of the mirror under multi-conditions, and the resilient connector was optimized by stress deconcentration and viscoelastic materials damping to obtain adequate dynamic strength margin. Finally, the comprehensive performance of the subassembly was verified eligible by finite element analysis that the mirror surface error RMS was superior to 0.002 λ under objective static conditions with enough safety margin in the harsh vibrations. In conclusion, the flexible support structure brought forward by this article is feasible which has general compatibility for other small-size space mirror.

Keywords: Space mirror · Support structure · Flexible hinge

1 Introduction

The optical mirror is the core component of the space remote sensor whose surface figure accuracy is of critical importance for the system's image quality. However, the surface fidelity usually suffers from static precision aberrations caused by gravitational release, thermal deformations, and alignment errors during the deployment or working procedure [1].

Therefore, developing a reasonable support structure is the key approach to achieve adequate mirror surface fidelity under multiple complex conditions [2]. The support structures generally involved can be divided into 3 types: lateral support, central support and bottom support, of which the first way is the simple one that is often adopted for

mirrors of small aperture. Typically, the mirror is set in a metal ring-type substrate and rigidly mounted on the main frame. But when the mirror's size increases to 260 mm or greater, this strategy can hardly meet the requirements on the mirror's surface precision claimed by the optic system [3]. In order to reduce the surface error brought by temperature and assembly as well as ensure adequate strength to stick up to gravity effect and dynamic environment, research about different kinds of flexible mirror support structure were carried out successively [2–6].

In this article, a Φ260 mm-diameter space mirror was expected to maintain surface figure error root mean square (RMS) at the high precision of less than λ/60 and survive in launch vibrations at the same time, thus the idea of combing lateral support with flexible mounting structure was proposed and a vibration mitigation method by application of the viscoelastic damping adhesive was studied. Finally, the whole approaches were verified by the finite element method to be effective and satisfactory.

2   Conventional Lateral Support Structure

A typical method to laterally support the small mirror was using distributed adhesives to connect the mirror with an annular cell at the lateral side, see Fig. 1. The mirror subassembly consisted of mirror, annular cell, axial clamps, radial glue spots and axial glue spots. The mirror was upholded by the cell through the radial glue while the axial glue only worked to limit the moving range for protection [7].

Usually, the cell was made of titanium alloy and the clamps were connected to the main frame rigidly. Under this circumstance, when temperature goes up or down, the mirror will be strongly dragged by the cell to expand or contract as the coefficient of thermal expansion (CTE) of the two was rather different, and when the subassembly is mounted with inevitable alignment error or the fitting surface deforms, the mirror will also be strongly forced to distort. All these factors may cause surface figure degradation of the mirror.
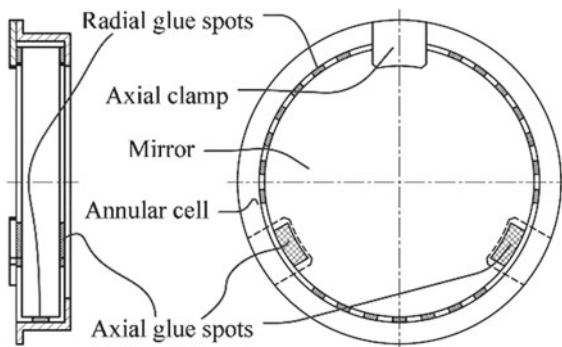

Fig. 1. Typical mirror support structure.

3   Study of the Flexible Support Structure

3.1   Research Goal

The mirror discussed in this paper is 260 mm in diameter which was required to keep the surface figure RMS superior to $1/60\lambda$ ($\lambda = 632.8$ nm) throughout the whole lifecycle and withstand the launch vibrations without plastic deformation or failure.

The working conditions taken into consideration include: (1) 1G (9.8 m/s^2) gravity in the assembly direction; (2) Temperature rise of 5 °C; (3) 0.02 mm translational or 10" rotational aberration of the fitting surface; (4) Target level of random vibration.

With such high precision demand, the goal of this paper is to reduce the surface error RMS caused by (1) ~ (3) to less than 0.002λ and ensure the stress safety margin of all parts to be higher than (3 in 4).

3.2   Kinematic Support Principle

To largely release the distortion stress passed from the main frame, the kinematic support method was investigated. As Fig. 2 presents, the mirror-cell-clamp (MCC) module was mounted on the main frame through three connectors. In order to set the module at a determinate position free of redundant restrictions, a statically determinate structure with zero degree of freedom (DOF) was proposed.
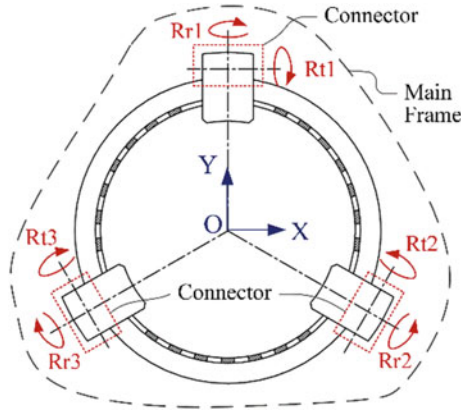

Fig. 2. 2 DOF of the MCC's connector.

The DOF of the spatial mechanism without general constraint is shown as follow [8]

$$W = 6(n-1) - \sum_{k=1}^{5}(6-k)P_k \tag{1}$$

where W denotes the whole DOF of the mechanism, $(n-1)$ denotes the number of moving parts, P_k denotes the number of k-level kinematic pair and k denotes the number

of kinematic pair's constraints. As for the mirror subassembly in Fig. 2, each connector has a 2 DOF motion pair with the revolving DOF Rt and Rr which takes on 4 constraints. Therefore, $P_1 \sim P_3$, $P_5 = 0$, $P_4 = 3$, and $(n - 1) = 1$. It can be deduced that the MCC's DOF is zero which can meet the requirements for exact restriction.

3.3 Preliminary Design

3.3.1 Structure Composition

Due to the inevitable frictions, fit clearance, transmission error and creep issues of the rigid motion pairs would greatly increase the design complexity and impair the system accuracy [9], the specially designed resilient connector which could realize high-precision movement in a small range [10] will be used to simulate the required rotational DOF. The mirror subassembly consisted of the MCC module and three resilient connectors, which adopted 2 orthogonal circular-arc flexible hinges to simulate the 2 rotational DOF with relatively high rigidity and good machining accuracy, see Fig. 3.
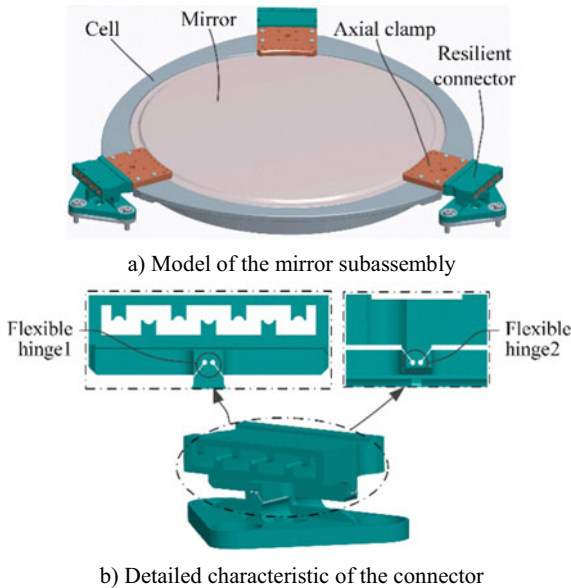

a) Model of the mirror subassembly

b) Detailed characteristic of the connector

Fig. 3. Preliminary structure composition

3.3.2 Material Selection

The silicon carbide (SiC) ceramics has relatively high rigidity, low CTE, moderate density and good dimensional stability, so it was choosed as the mirror material to design a lightweight and stable optical element. To reduce the optical distortion caused by the mirror and cell's inconsistent expansion or contraction, materials of both need to be thermal adaptive. Carbon fiber reinforced silicon carbide ceramic matrix (C/SiC)

composites, as a promising structural material in the aerospace field, has relatively high specific strength with CTE close to the SiC ceramics. So, it was chosen as the cell material to provide reliable and compliant support for the mirror.

As the other parts were not joint with the mirror directly and expected to be high-strength and lightweight, so the titanium alloy was chosen in synthetical consideration.

Materials of the main components of the mirror subassembly and their detailed performance parameters are listed in detail in Table 1. In a whole, the mirror subassembly only weighs 2.1 kg.

Table 1. Performance parameters of materials.

Material	Elastic modulus E/(Gpa)	Poisson's ratio μ	Density ρ/(g/cm^3)	CTE α/(μK^{-1})
SiC	350	0.17	3.12	2.5
C/SiC	70	0.3	2.5	1.6
Titanium alloy	110	0.32	4.5	9.1

3.3.3 Mounting Principles

Based on the flexible support structure, a micro-stress mounting strategy was proposed to further reduce the initial discomfort of the mirror brought by assembly. The overall idea is firstly, fit the MCC module to the main frame at the theoretical position through a special non-contact tooling, secondly locate the connectors by the corresponding clamp and assemble them to the main frame with bolts, then remove all the temporary toolings, finally inject the glue filler to the jagged clearance through the injection channels and holes with the help of the dedicated tooling and wait the glue filler became dry, see Fig. 4. That is, the clamps and connectors will join with tiny stress.

3.3.4 Parameter Design of the Flexible Hinge

The parameters of the flexible hinge are associated with the bracing stiffness of the connector which need to be suitable to resolve the conflict between error unloading capability and dynamic carrying capacity. The rotational stiffness of the circular-arc flexible hinge K is the key to design which can be expressed as [11]
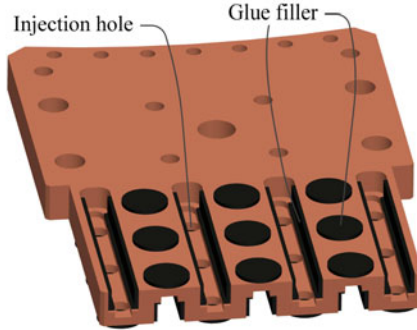
$$K = M_z/\alpha_z \approx \left(2Ebt^{5/2}\right)/\left(9\pi R^{1/2}\right) \tag{2}$$

where M_z denotes the torque exerted on the hinge, α_z denotes the rotation angle of the hinge, E denotes the material's elastic modulus, b denotes the width of the hinge, t denotes the thickness of the thinnest place of hinge section, and R denotes the radius of the circular arc, see Fig. 5.

According to Eq. (2), the argument t impacts most which need to be focused on in subsequent optimization. Therefore, the value of b and R were pre-set based on
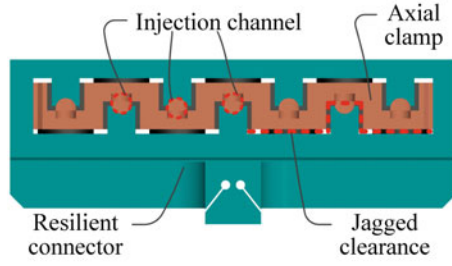
a) Make up of the clamp-conncetor module

b) The reselient connector hidden

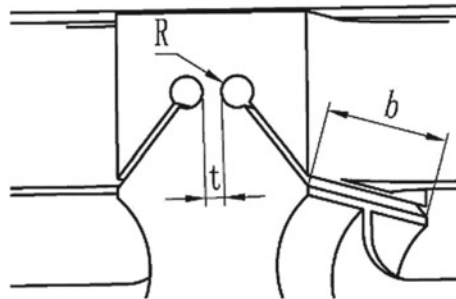**Fig. 4.** Assembly elements of the clamp-connector module.

Fig. 5. Parameters of the circular-arc hinge.

the structure size and process requirements. Suppose b_i, R_i and t_i denotes the relative parameters of the flexible hinge i (see Fig. 3), $b_1 = 28$ mm, $b_2 = 48$ mm, and $R_1 = R_2 = 0.5$ mm. With the aid of finite element analysis (FEA), the optimal value of t_1 and t_2 were finally found at 0.6 mm to meet the forced displacement unloading need.

4   Analysis and Improvement

4.1   Static Precision Analysis

To show the beneficial effects of the support structure proposed by this paper, the surface error RMS of the following two types of mirror subassembly were analyzed by the FEA method respectively: (A) Typical type: the subassembly fitted with hard link, using the titanium alloy cell; (B) New type: the subassembly fitted with the special resilient connectors, using the C/SiC cell.

Then the following 5 working conditions were simulated (based on Fig. 6): (a) A ~ C fixed with 1G gravity along -Y; (b) A ~ C fixed with temperature rise of 5 °C; (c) B and C fixed while A was given 0.02 mm displacement + Z; (d) B and C fixed while A was given 10" displacement about + X; (e) B and C fixed while A was given 10" displacement about + Y.
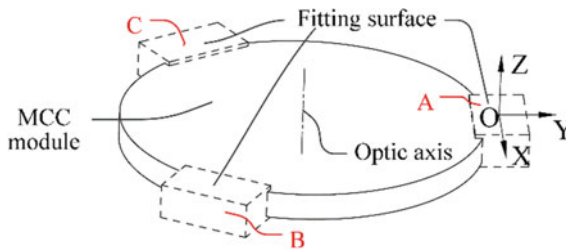

Fig. 6. Definition of the simulation.

By simulation, the mirror's surface figure RMS was obtained, see Table 2. Clearly that the typical type cannot fit the bill in the (b), (c) and (e) conditions with RMS error greater than the requested 0.002λ, while the new type structure behaved as expected whose results all satisfied the demand.

Table 2. Surface RMS of the 2 types in 5 working conditions.

RMS /λ	(a)	(b)	(c)	(d)	(e)
(A)	0.00059	0.00469	0.00690	0.00010	0.00304
(B)	0.00080	0.00155	0.00017	0.00002	0.00009

4.2 Dynamic Strength Analysis

The constraint modal of the subassembly was carried out based on FEA and the fundamental frequency was found at 118 Hz showing as the mirror's translation along the optical axis. Then, the frequency response in 3 directions from 20 to 2000 Hz was simulated. Overall, the Z-direction response at 118 Hz manifested as the harshest condition which has the highest stress level.

On this basis, the random response of acceleration and stress under given level of random vibration (5G RMS from 20 to 2000 Hz) was obtained. Overall, there was only one risk area of the subassembly (see Fig. 7) whose Von-Mises stress level was high to the yield limit. The maximum stress RMS appeared at the section center of the flexure hinge and reached 258 Mpa. According to the 3σ clipping rule [12], the maximum stress was 774 Mpa, close to the titanium alloy's yield limit 810 Mpa. Therefore, the safety margin is inadequate and need to be improved urgently.
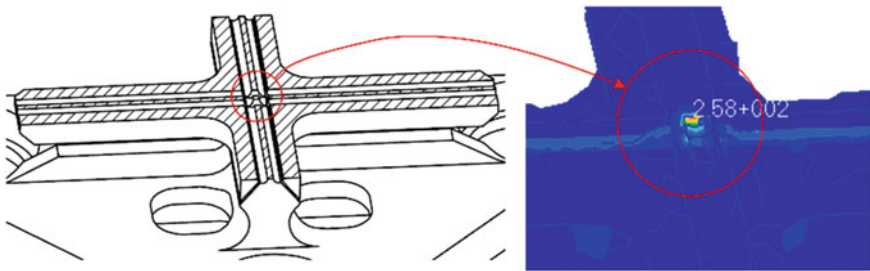

Fig. 7. Maximum stress area of the resilient connector.

4.3 Improvement

The stress concentration and the flexure design caused high stress level in the connector which could be solved following the two ideas: (a) removing the materials of the stress concentration region; (b) adopting the damping anti-vibration method.

In terms of the first approach, a hole cutting through the flexure hinge centre was set which removed the top 80% high stress solid, see (a) in Fig. 8. For the second approach, shear deformation occurred in the viscoelastic damping materials to turn the vibration mechanical energy into heat and dissipate, thus to reduce the response [13]. The viscoelastic materials' low elastic modulus and high shear loss factor in specific temperature and frequency are critical parameters for the damping effect [14]. In order to take full advantage of the shear properties of the damping material, the adhesive was arranged along the tangent of the flexure hinge to bear the shear force, see (b) in Fig. 8.

By calculation, the maximum stress of the resilient connector was reduced to 243Mpa (based on 3σ rule) with safety margin of 3.33 which verified the subassembly's dynamic strength to be eligible.
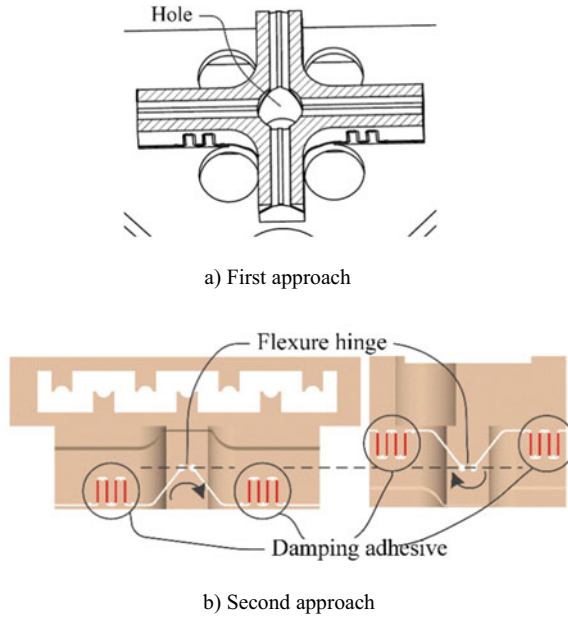
a) First approach

b) Second approach

Fig. 8. Improvement of the resilient connectors.

4.4 Recheck of the Static Precision

The improved structure's static precision related with gravity, temperature and assembly need to be re-assessed in the conditions same as Sect. 4.1. Table 3 compares the surface figure error RMS of the original and the improved structure. It can be verified that the improvement didn't cause bad impact on the static precision of the subassembly and the modified scheme was feasible.

Table 3. Surface RMS of the original and improved structure.

RMS /λ	Gravity	Temp	0.02 mm along + Z	10" about + X	10" about + Z
Original	0.00080	0.00155	0.00017	0.00002	0.00009
Improved	0.00125	0.00155	0.00003	0.00001	0.00013

5 Conclusion

This paper studied the flexible support structure for a Φ260mm-diameter space mirror. In order to suffice the comprehensive requirements of static precision and dynamic strength under multi-conditions, a statically determinate discrete support scheme was proposed based on the kinematic analysis method, combining the conventional ring-type

lateral support structure with resilient connectors disposed at the periphery. Targeting at minishing the optical degradation against thermal variation and forced displacement from the fitting area, parameters of the connector's flexure hinge were optimized, and the micro-stress mounting strategy was applied while materials of the mirror and cell were creatively chosen to be CTE consistent. Later, the comprehensive performance related with gravity, temperature and assembly was evaluated to be eligible. As the safety margin in random vibration was insufficient, the resilient connector was optimized to be stress deconcentrated and damp-increased with viscoelastic materials, which notably improved the safety margin to be eligible with undisturbed error unloading capability. The flexible support structure put forward by this paper is of reference meaning for design of other the small-size space mirror subassembly.

References

1. Rausch P, Verpoort S, Wittrock U (2015) Unimorph deformable mirror for space telescopes: design and manufacturing. Opt Express 23(15):19469–19477
2. Wang ZS, Zhai Y, Mei G et al (2010) Design of flexible support structure of reflector in space remote sensor. Opt Precis Eng 18(8):1833–1841
3. Wang WP, Lv TY, Liu XY et al (2019) Flexure support design and optimization for middle-small spherical mirror. J Chang Univ Sci Technol 42(3):7–10
4. Liu M, Zhang LZ, Li X et al (2018) Design of flexure support of space compact reflector subassembly and dynamic analysis. Opto-Electron Eng 45(5):1–10
5. Wang ZS, He X, Fu LL (2011) Design and analysis for a minitype mirror supporting structure. Opt Tech 37(6):686–690
6. Li YP, Wang Z, Sha W et al (2018) Structural design of primary mirror subassembly for spatial gravitational wave telescope. Infrared Laser Eng 47(8):1–7
7. Luo SK, Cao DJ, Lan LY et al (2016) Support technique of space mirror based on diversity between apparent Young modulus and shear modulus. Spacecr Recover Remote Sens 37(1):41–47
8. Zhang YX, Chen DS, Liao ZF et al (2003) Exploration on the formula of degree of freedom of space mechanism. J Chongqing Univ 26(9):53–55
9. Shi RC (2013) Optimal design and system development of a flexible parallel high-precision pointing mechanism [D]. Harbin: Harbin Institute of Technology
10. Tseytlin Y (2012) Note: rotational compliance and instantaneous center of rotation in segmented and V-shaped notch hinges. Rev Sci Instrum 83(2):026102
11. Yang SY (2008) Analysis of geometrical parameters of circular arc flexible hinge influence on its rigidity. Coal Mine Mach 29(7):81–82
12. Zhu XW, Zhang SJ, Ning ZG et al (2014) Applications of 3σ clipping rule in the fatigue damage accumulation analysis. Spacecr Environ Eng 31(6):609–613
13. Baker M (2007) Analysis method to support design for damping. Eng Comput 23(1):1–10
14. Qiu JH, Fan B, Lian HD (2015) Research on the application of viscoelastic constrained layer damping in space large aperture mirror. Spacecr Recover Remote Sens 36(2):32–38